2017

# Fracture toughness measurement for aluminium 6061-T6 using notched round bars

Alan K. Hellier
*University of Wollongong*, ahellier@uow.edu.au

P Chaphalkar
*University of New South Wales*

Gangadhara B. Prusty
*University of New South Wales*, g.prusty@unsw.edu.au

# Fracture toughness measurement for aluminium 6061-T6 using notched round bars


## Abstract

Current standard testing methods for determining plane strain fracture toughness (KIc), such as ASTM E399 and ASTM E1820, require a prior estimate of KIc, plus the specimens are large, involve a lot of machining and need fatigue pre-cracking. There is therefore a desire to develop new testing techniques which are simple, as well as cost and time effective. While the use of tensile notched round bar (NRB) test pieces is not novel, dating back to a conference paper by Brown in 1975, relatively few authors have so far attempted this. A series of such tests has been conducted on aluminium 6061-T6 NRB specimens having various notch root radii of 0.5mm, 0.8mm, 1.0mm, 1.2mm and 1.5mm. The inner neck diameter at the notch plane d and the outer specimen diameter D were standard values, being the same for all tests. No fatigue pre-cracking was carried out. Graphs of apparent fracture toughness K versus the 'notch bluntness ratio' 1 = / d were extrapolated to zero, corresponding to a fatigue pre-cracked configuration. A recently proposed 'geometric correlation' 2 based on , d and D was also utilised to linearly extrapolate K values, measured on NRB specimens with arbitrary geometries (but assuming plane strain conditions hold), back to a single value of KIc: The stress concentration factor (Kt) at the notch root was determined in each case using two different methods: two-dimensional axisymmetric finite element analysis, and additionally theoretical values calculated using the equations of Roark. The finite element analyses exhibited a singularity at the notch root, so it was necessary to fit a straight line to the central portion of the h-convergence stress curve and extrapolate this to the notch root. Use of the 'geometric correlation' and theoretical Kt values resulted in a conservative KIc value (26.8 MPam) close to the established literature value of 29 MPam, an error of -7.5%. The main purpose of this paper is to help build evidence for the future standardisation of the NRB test piece.



## Disciplines

Engineering | Science and Technology Studies

## Publication Details

Hellier, A. K., Chaphalkar, P. P. & Prusty, B. G. (2017). Fracture toughness measurement for aluminium 6061-T6 using notched round bars. 9th Australasian Congress on Applied Mechanics (ACAM9) (pp. 332-339). Sydney: Engineers Australia.

# Fracture Toughness Measurement for Aluminium 6061-T6 using Notched Round Bars

A.K. Hellier[1], P.P. Chaphalkar[2] and B.G. Prusty[2]
[1]School of Mechanical, Materials, Mechatronic & Biomedical (MMMB) Engineering
University of Wollongong
Northfields Avenue
Wollongong, NSW 2522
AUSTRALIA
[2]School of Mechanical & Manufacturing Engineering
UNSW Australia (The University of New South Wales)
Sydney, NSW 2052
AUSTRALIA
E-mail: alanhellier@optusnet.com.au

***Abstract:*** *Current standard testing methods for determining plane strain fracture toughness ($K_{Ic}$), such as ASTM E399 and ASTM E1820, require a prior estimate of $K_{Ic}$, plus the specimens are large, involve a lot of machining and need fatigue pre-cracking. There is therefore a desire to develop new testing techniques which are simple, as well as cost and time effective. While the use of tensile notched round bar (NRB) test pieces is not novel, dating back to a conference paper by Brown in 1975, relatively few authors have so far attempted this. A series of such tests has been conducted on aluminium 6061-T6 NRB specimens having various notch root radii $\rho$ of 0.5mm, 0.8mm, 1.0mm, 1.2mm and 1.5mm. The inner neck diameter at the notch plane d and the outer specimen diameter D were standard values, being the same for all tests. No fatigue pre-cracking was carried out. Graphs of apparent fracture toughness $K_\rho$ versus the 'notch bluntness ratio' $\alpha_1 = \rho / d$ were extrapolated to zero, corresponding to a fatigue pre-cracked configuration. A recently proposed 'geometric correlation' $\alpha_2$ based on $\rho$, d and D was also utilised to linearly extrapolate $K_\rho$ values, measured on NRB specimens with arbitrary geometries (but assuming plane strain conditions hold), back to a single value of $K_{Ic}$:*

$$K_\rho \propto \sqrt{\rho\,(D-d)\,/\,D^2}$$

*The stress concentration factor ($K_t$) at the notch root was determined in each case using two different methods: two-dimensional axisymmetric finite element analysis, and additionally theoretical values calculated using the equations of Roark. The finite element analyses exhibited a singularity at the notch root, so it was necessary to fit a straight line to the central portion of the h-convergence stress curve and extrapolate this to the notch root. Use of the 'geometric correlation' and theoretical $K_t$ values resulted in a conservative $K_{Ic}$ value (26.8 MPa√m) close to the established literature value of 29 MPa√m, an error of -7.5%. The main purpose of this paper is to help build evidence for the future standardisation of the NRB test piece.*

***Keywords:*** *Aluminium 6061-T6, notched round bar specimen, axisymmetric finite element analysis, stress concentration factor, plane strain fracture toughness.*

## 1. INTRODUCTION

Solutions to the stress concentration problem of a cylindrical bar with a circumferential V-shaped groove are mainly used in practice for the design of shafts. Stress concentration factors ($K_t$) and stress intensity factors ($K_I$) are also important for test specimens used to investigate the fatigue strength of a metal [1,2]. Following the 1984 paper [1], a circumferentially notched tension (CNT) test piece was developed by Stark and Ibrahim [3] as a smaller plane strain fracture toughness ($K_{Ic}$) test piece than is allowed by the current standards, ASTM E399 [4] and E1820 [5], which make use of either compact tension (CT) or single-edge-notched bend (SENB) test pieces. These standard tests are elaborate, complex and costly.

Finite element (FE) studies on fatigue pre-cracked round bar specimens confirmed that the CNT specimen geometry, even if of a very small size, often ensures plane-strain conditions for a fracture

toughness test. These FE studies [6] indicated that the fatigue crack should be at least twice the Irwin plastic zone correction factor in depth; if shallower than that, the result tended towards the higher plane stress result. In order that general yielding of the final ligament at fracture be avoided, the average stress across the ligament at fracture should not exceed 2.5 times the yield strength of the material. In the event that this limit is exceeded, then a larger specimen diameter would be required [6]. However, the stress concentration factor $K_t$ of the notch is not of critical importance, as it is only there to facilitate the growth of a uniform fatigue pre-crack under rotating-bending loading. Such specimens are subsequently tested in tension and have been used, for example, to investigate sustained-load fracture at stress intensity factors $K_I$ less than $K_{Ic}$ in the neck of aluminium 6061 and 6351 gas cylinders [7]. Londe et al. [8] have used a very similar test piece, which they have dubbed the circumferentially cracked round bar (CCRB), to obtain a valid $K_{Ic}$ for Al 6082-T6. Donoso and Labbe [9] have shown from nonlinear numerical analysis of notched (pre-cracked) cylindrical specimens that a plane strain to plane stress tendency occurs when the ratio $d$ / $D$ exceeds about 0.5 (where $d$ is the diameter of the notch and $D$ is the outer specimen diameter). Li and Bakker [10] have used the ASTM standard *J–R* testing procedure on such a pre-cracked NRB specimen to get a value of the ductile fracture toughness $J_{Ic}$.

Wu [11] has proposed a single smooth round bar tensile specimen (with no notch or pre-crack) method of determining $K_{Ic}$ for a ductile metal, with an error of better than 5%. It relies on dividing the tensile diagram into two parts: the loading curve and the fracture curve. For brittle metals, an artificial circumferential pre-crack is required. This is probably the simplest and cheapest method for measuring $K_{Ic}$, and is independent of specimen diameter (provided the latter lies between 10–15mm). Oh [12] has applied the dynamic fatigue-life equation to the elastic-plastic deformation in the uniaxial tensile test. The surface energy per unit area is proportional to the ratio of the plastic and elastic elongation. The calculated fracture toughness values for annealed 4340 steel, Al 2024-T3 and Al 7075-T6 using this method coincided very well with the ASTM E399 values.

Brown [13] appears to be the first to have used uncracked circumferentially notched round bars (NRB) with finite notch root radii to determine $K_{Ic}$ values. Also Wilson and Landes [14,15], based on work from a PhD thesis by Wilson [16], have further developed this method which has been used in the present work. This paper is based on work originally reported in a Coursework Masters thesis by Chaphalkar [17]. The latter is held in UNSWorks and is downloadable from the UNSW Library.

## 2. EXPERIMENTAL METHODS

### 2.1. Experimental Material

Aluminium 6061 exhibits excellent joining characteristics and good acceptance of applied coatings, combines relatively high strength with good workability and high resistance to corrosion, and is also widely available [18]. Its applications include the following: aircraft fittings, camera lens mounts, couplings, marine fittings and hardware, electrical fittings and connectors, decorative or miscellaneous hardware, hinge pins, magneto parts, brake pistons, hydraulic pistons, appliance fittings, valves and valve parts, bike frames [18].

Table 1 Literature mechanical properties of aluminium 6061-T6 alloy [18]

| **Property** | **Al 6061-T6** |
|---|---|
| Young's modulus | 68.9 GPa |
| Poisson's ratio | 0.33 |
| Tensile yield stress | 276 MPa |
| Ultimate tensile strength | 310 MPa |
| Elongation at break for 12.7mm (1/2 in.) diameter | 17% |
| Brinell hardness | 95 |
| Fracture toughness $K_{Ic}$ (T-L orientation) | 29 MPa$\sqrt{m}$ |

The stock material used for the present work was a solid round bar 25.4mm (1 inch) in diameter and 4m in length. Since no material test certificate was available from the supplier, the general property values given by the ASM [18] and reproduced in Table 1 are considered in the first instance to be acceptable theoretical values for use in this work.

## 2.2. Experimental Methodology

The methodology employed in the current work may be divided into three major parts.

The first part involved the tensile testing of smooth round bar specimens in order to obtain the tensile properties of the material. This was followed by the tensile testing of notched round bars of the same material having different notch root radii, $\rho$. This was done to obtain the fracture strength of the material for different notch geometries. A summary of all the specimen geometries selected for testing is given in Table 2. The notch angle was 60° in all cases. *D* is the outer diameter of the specimen, and *d* is the inner neck diameter of the specimen at the notch plane, or remaining ligament.

Table 2 Summary of specimen geometries chosen for tensile testing

| **Material** | **Test Type** | ***D* (mm)** | ***d* (mm)** | **$\rho$ (mm)** | **Designation** |
|---|---|---|---|---|---|
| Al 6061-T6 | Smooth | 10 | 10 | – | T1, T2, T3 |
| | Notched | 14 | 10 | 0.5 | N051, N052, N053 |
| | | 14 | 10 | 0.8 | N081, N082, N083 |
| | | 14 | 10 | 1.0 | N101, N102, N103 |
| | | 14 | 10 | 1.2 | N121, N122, N123 |
| | | 14 | 10 | 1.5 | N151, N152, N153 |

The specimens were manufactured and tested according to AS 1391:2007 [19]. The tensile testing for both the smooth and notched specimens was performed on an INSTRON 3369 dual column table-top testing machine which had a rating of 50 kN. The rate of applied loading was 2mm/min. Figure 1 contains a drawing of the smooth tensile specimen as well as one of the notched round bar specimens.

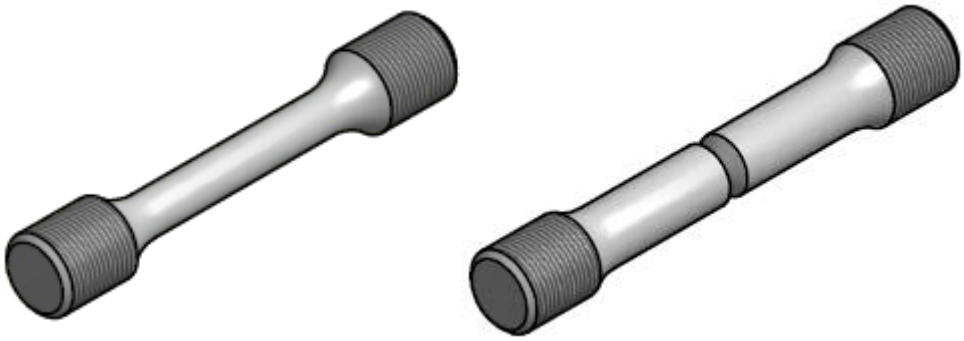

Figure 1 – Drawing of a smooth tensile specimen and one of the notched round bar specimens.

The second part of the analysis involved developing a finite element (FE) model, based on the specimen geometry and material properties obtained through the first testing part. Each FE model is a 2-D axisymmetric mesh, which consists of one quarter of the actual test specimen. This symmetry saves a great deal of computational time. The FE analysis is performed in order to obtain the maximum stress occurring in the material, in the vicinity of the notch, before it fractures. A linear-elastic stress analysis approach is used to determine the maximum fracture stress [17]. The latter is then divided by the applied fracture stress to obtain an estimate of the stress concentration factor, $K_t$. Alternatively, the theoretical stress concentration factor may be obtained from the literature, for example using the well-known equations due to Roark [20].

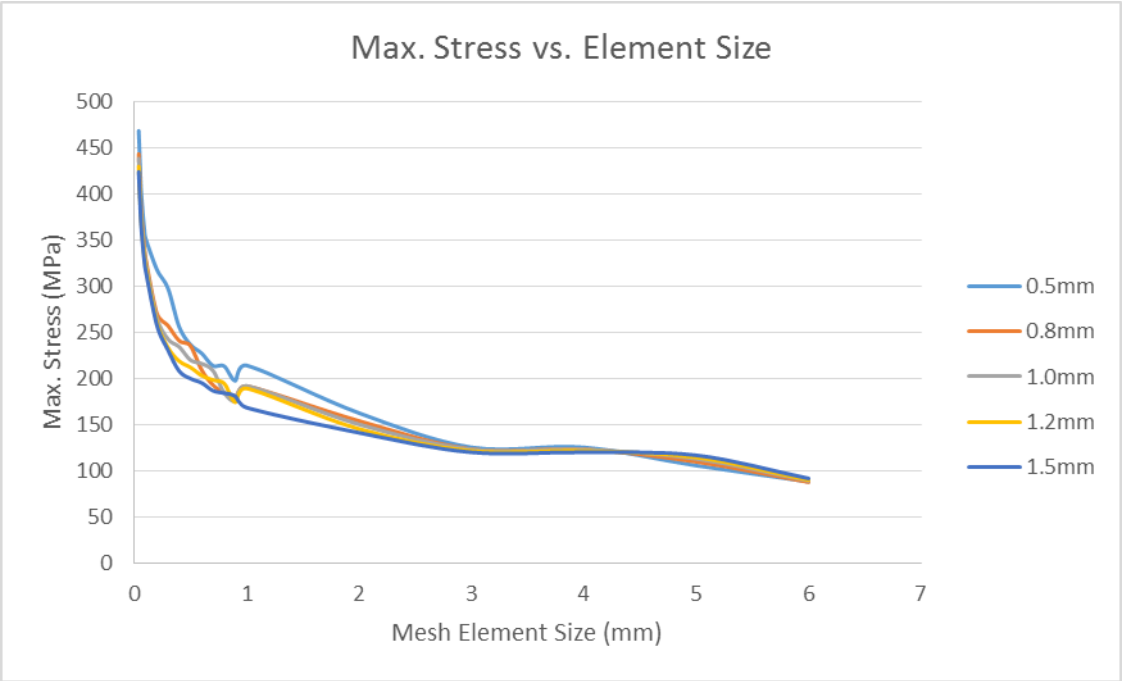


Figure 2 – h-convergence results for quadrilateral elements containing midside nodes.

Convergence tests were performed to verify the quality of the computational results using quadrilateral elements containing midside nodes. The element size was varied between 6mm and 0.04mm. The results are shown for each notch root radius in Figure 2 above. This shows that the maximum stress varies considerably for the lowest element sizes. This is due to the fact that the linear elastic stress analysis does not consider the effects of localised plasticity due to the presence of high stresses near the crack tip. Hence as the element size decreases, the computed values are closer to the notch root leading to a singularity or infinite stress. These stress values are to be avoided in the current calculation as they are meaningless. From Figure 2 it may be seen that the maximum stress does not change much for mesh sizes between 2mm and 6mm. A least squares regression analysis was therefore performed and a linear curve fit was applied within this range, in order to estimate the true value for the maximum stress before fracture for a particular notch root radius.

The third part of the analysis uses the results obtained from the first two parts as inputs to find initially the stress concentration factor ($K_t$) followed by calculation of the stress intensity factors using Irwin's [21] limit equation (see (1) below) and finally the results would be used to compute the plane strain fracture toughness of the material by extrapolating the values of stress intensity factors for different notch root radii to zero:

$$K_{Ic} = \lim_{\rho \to 0} \left( \frac{1}{2} K_t \sigma_f \sqrt{\pi \rho} \right) \qquad (1)$$

The apparent fracture toughness curve is constructed by plotting the $K_\rho$ values found for different notch root radii against the 'notch bluntness ratio' $\rho / d$ ($\alpha_1$) proposed by Shabara et al. [22] or the 'geometric correlation' parameter ($\alpha_2$) as developed by Vanian et al. [23]:

$$K_\rho \propto \sqrt{\rho \, (D - d)} \, / \, D^2 \qquad (2)$$

where $D - d$ is proportional to the notch (crack) length and $D^2$ is proportional to the cross-sectional area of the specimen at its ends. Use of this relationship removes the influence of specimen geometry on $K_\rho$. This should enable the extrapolation of $K_\rho$ results obtained from NRB specimens with any arbitrary values of the geometric parameters $\rho$, $d$ and $D$, along the same straight line to give an estimate of $K_{Ic}$ (provided plane strain conditions apply in each case).

## 3. RESULTS AND DISCUSSION

The results of the tensile tests on all three plain tensile specimens T1, T2 and T3 are contained in Table 3 below. The deviations from the ASM literature data [18] set out in Table 1 are also given. As expected, optical microscopy showed failure was highly ductile by cup-and-cone rupture in each case.

Table 3 Tensile test results from uniaxial tension tests on actual aluminium 6061-T6 alloy specimens

| **Tensile Property** | **T1** | **T2** | **T3** | **Mean** | **ASM Data Value** | **Deviation** |
|---|---|---|---|---|---|---|
| Maximum load (kN) | 29.44 | 29.72 | 29.31 | 29.49 | – | – |
| Ultimate tensile strength (MPa) | 374.95 | 378.41 | 373.17 | 375.51 | 310 | +21% |
| 0.2% offset yield stress (MPa) | 356.5 | 357.78 | 353.96 | 356.08 | 276 | +29% |
| Modulus of elasticity (GPa) | 69.4 | 71.4 | 70.5 | 70.4 | 68.9 | +0.2% |
| Poisson's ratio | 0.3261 | 0.3437 | 0.3274 | 0.3324 | 0.33 | +0.1% |

As can be seen from Table 3, the deviation in the yield stress and ultimate tensile strength indicates that the experimental material has a higher strength as compared to literature values. This variation of about 20–30% was confirmed by the supplier CAPRAL to be present due to the fact that each batch is solution heat treated according to specific procedures related to the Al 6061-T6 alloy, but variations do exist, and the changes in material properties occur due to uneven heat treatment temperatures. The strength may be reduced or increased due to this variation. The properties available from the literature are considered to be the minimum desired properties for the alloy and hence, since the current values are above the minimum ones, they may be considered generally acceptable (as stated by CAPRAL).

The apparent fracture toughness curve is constructed by plotting the $K_\rho$ values found for different notch root radii against either the 'notch bluntness ratio' ($\alpha_1$) or the 'geometric correlation' parameter ($\alpha_2$). Table 4, which follows, summarises the values of $\alpha_1$, $\alpha_2$, $K_t$ and $K_\rho$ for all the different notch root radii. $K_t$ and $K_\rho$ here were calculated using the FE linear curve fit and extrapolation method [17]. Failure was ductile (macroscopically flat but with pronounced crack propagation 'ridges') in all cases.

Table 4 Apparent fracture toughness data

| $D$ (mm) | $d$ (mm) | $\rho$ (mm) | $\alpha_1$ | $\alpha_2$ | $K_t$ | $K_\rho$ (MPa√m) |
|---|---|---|---|---|---|---|
| 14 | 10 | 0.5 | 0.05 | 0.007215 | 4.09 | 42.9 |
| 14 | 10 | 0.8 | 0.08 | 0.009127 | 3.43 | 44.6 |
| 14 | 10 | 1.0 | 0.10 | 0.010204 | 3.32 | 48.3 |
| 14 | 10 | 1.2 | 0.12 | 0.011178 | 3.20 | 50.8 |
| 14 | 10 | 1.5 | 0.15 | 0.012497 | 3.05 | 54.4 |

Plots were produced of the apparent fracture toughness $K_\rho$ for different notch root radii $\rho$ plotted against the 'notch bluntness ratio' ($\alpha_1$) and 'geometric correlation' ($\alpha_2$). Once plotted, least squares regression was used to add a line of best fit. The extrapolated value of the vertical axis intercept of this line gives the Mode I plane strain fracture toughness of the material ($K_{Ic}$). Figure 3 shows one such plot.

Table 5, which follows, summarises the fracture toughness results obtained using both the FE linear curve fit and extrapolation method [17] and the theoretical formula method [20] for calculating $K_t$. Also used with both of these is the 'notch bluntness ratio' ($\alpha_1$) as well as the 'geometric correlation' ($\alpha_2$).

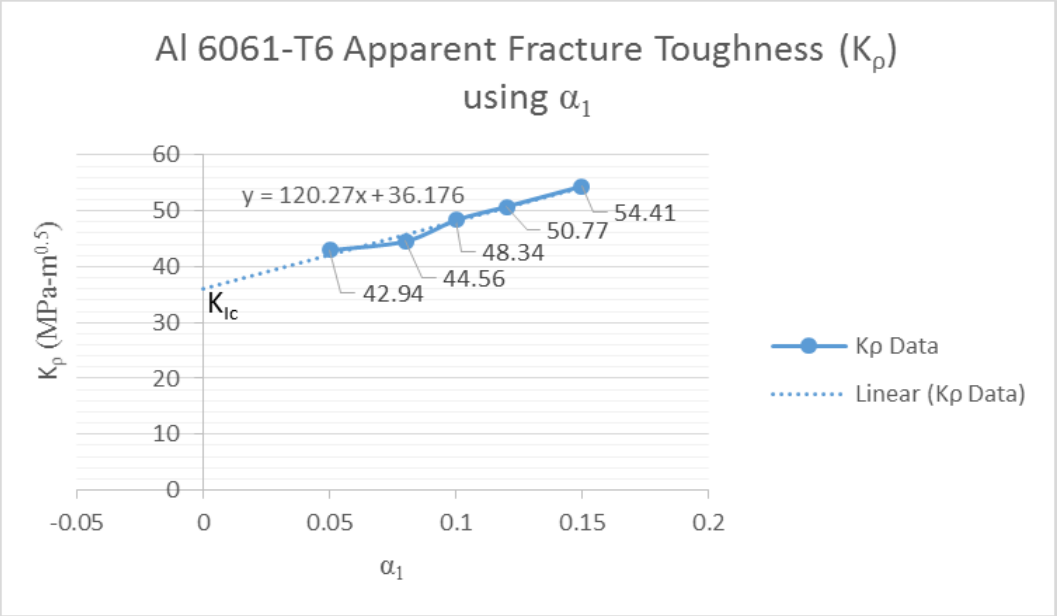


Figure 3 – Graph of apparent fracture toughness $K_\rho$ versus 'notch bluntness ratio' $\alpha_1$.

Table 5 Summary of fracture toughness results

| ***$K_t$* Calculation Method** | **Parameter** | **Established *$K_{Ic}$*** | **Measured *$K_{Ic}$*** | **Deviation** |
|---|---|---|---|---|
| FE linear curve fit and extrapolation [17] | 'Notch bluntness ratio', $\alpha_1$ | 29 MPa√m | 36.2 MPa√m | +24.8% |
| | 'Geometric correlation', $\alpha_2$ | 29 MPa√m | 25.6 MPa√m | -11.7% |
| Theoretical formula (Roark) [20] | 'Notch bluntness ratio', $\alpha_1$ | 29 MPa√m | 29.9 MPa√m | +3.1% |
| | 'Geometric correlation', $\alpha_2$ | 29 MPa√m | 26.8 MPa√m | -7.5% |

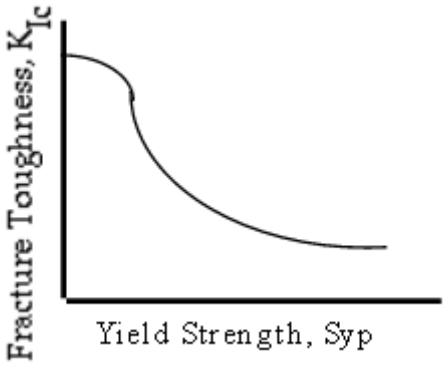


Figure 4 – Schematic showing variation of fracture toughness $K_{Ic}$ with yield strength [24].

As seen in Table 5 above, the measured $K_{Ic}$ value obtained using the theoretical stress concentration factor formula due to Roark together with the 'geometric correlation' gave the best result (being slightly conservative) although at first sight not the most accurate. However, taking into account the inverse relationship between yield stress and fracture toughness – see Figure 4 [24], and the fact that the experimental alloy had higher strength properties than those found in the literature (refer to Table 3), then this $K_{Ic}$ value is likely the most accurate as well. There is some inherent error in the slope of a line fitted to the central portion of the h-convergence stress curve. Fitting the line between mesh sizes of 2mm to 6mm is somewhat arbitrary and may result in some underprediction or overprediction of the true maximum stress. Roark's equations, on the other hand, give a single value of stress

concentration factor.

## 4. CONCLUSIONS

The singularity problem occurring with stress at the notch tip reaching infinity is seen clearly in the h-convergence study done by reducing the mesh element size for the modelled geometry. The line fit and extrapolation method employed in the nearly linear central region of the h-convergence plot has proven to provide an effective measure of the maximum stress, while avoiding the singularity problem.

It was also seen that the theoretical stress concentration factors calculated using Roark's equations produced accurate values using both the 'notch bluntness ratio' and the 'geometric correlation' to derive the fracture toughness of the material. The stress concentration factors derived from the FE linear curve fit and extrapolation method gave less accurate fracture toughness results. It is therefore recommended that Roark's equations be used in the future.

The 'geometric correlation' is preferred as it gave conservative fracture toughness results whereas the 'notch bluntness ratio' gave unconservative results.

Use of the 'geometric correlation' and theoretical $K_t$ values resulted in a conservative $K_{Ic}$ value (26.8 MPa$\sqrt{}$m) close to the established literature value of 29 MPa$\sqrt{}$m, an error of -7.5%. However, taking into account the inverse relationship between yield stress and fracture toughness, and the fact that the experimental alloy had higher strength properties than those found in the literature (refer to Table 3), then this $K_{Ic}$ value is likely the most accurate as well.

The NRB method for measuring $K_{Ic}$ has great potential and may in the future be amenable to standardisation, as has already been suggested for the Stark-Ibrahim CNT method. However, suitable specimen size requirements will first need to be established using FE analysis for the uncracked NRB geometry, as has already been done for the fatigue pre-cracked CNT test piece.

## 5. REFERENCES


1. Nisitani H, Noda N-A. Stress concentration of a cylindrical bar with a V-shaped circumferential groove under torsion, tension or bending. *Eng Fract Mech.* 1984;20(5/6):743-766.

2. Noda N-A, Takase Y. Generalized stress intensity factors of V-shaped notch in a round bar under torsion, tension, and bending. *Eng Fract Mech.* 2003 Jul;70(11):1447-1466.

3. Stark HL, Ibrahim RN. Estimating fracture toughness from small specimens. *Eng Fract Mech.* 1986;25(4):395-401.

4. ASTM Standard E399. Standard Test Method for Linear-Elastic Plane-Strain Fracture Toughness $K_{Ic}$ of Metallic Materials. West Conshohocken (PA): ASTM International; 2012. 33p

5. ASTM Standard E1820. Standard Test Method for Measurement of Fracture Toughness. West Conshohocken (PA): ASTM International; 2016. 53p

6. Ibrahim RN, Stark HL. Validity requirements for fracture toughness measurements obtained from small circumferentially notched cylindrical specimens. *Eng Fract Mech.* 1987;28(4):455-460.

7. Stark HL, Ibrahim RN. Crack propagation in aluminium gas cylinder neck material at constant load and room temperature. *Eng Fract Mech.* 1992 Mar;41(4):569-575.

8. Londe NV, Jayaraju T, Rao PRS. Use of round bar specimen in fracture toughness test of metallic materials. *Int J Eng Sci Technol.* 2010 Sep;2(9):4130-4136.

9. Donoso JR, Labbe F. *Q*-stresses and constraint behavior of the notched cylindrical tensile specimen. *Eng Fract Mech.* 2001 Mar;68(4):487-496.

10. Li DM, Bakker A. Fracture toughness evaluation using circumferentially-cracked cylindrical bar specimens. *Eng Fract Mech.* 1997 May;57(1):1-11.

11. Wu J-Q. A simple method for measuring $K_{IC}$ of ductile metals. *Eng Fract Mech.* 1992 Jan;41(1):1-5.

12. Oh H-K. Determination of fracture toughness by means of the uniaxial tensile test. *J Mater Proc. Technol.* 1995 Oct;54(1-4):372-374.

13. Brown WF Jr. The circumferentially notched cylindrical bar as a fracture toughness test specimen. Technical Paper presented at Symposium on Linear Fracture Mechanics. Bethlehem (PA): Lehigh University; 1974 Jul 29-30. In: Linear Fracture Mechanics. Lehigh Valley (PA): Envo Publishing Co.; 1975.

14. Wilson CD, Landes JD. Fracture toughness testing with notched round bars. In: Paris PC, Jerine KL, editors. Fatigue and Fracture Mechanics. 30th vol. West Conshohocken (PA): American Society for Testing and Materials; 2000. p. 69–82.

15. Wilson CD, Landes JD. Transition fracture toughness testing with notched round bars (NRB). In: Halford GR, Gallagher JP, editors. Fatigue and Fracture Mechanics. 31st vol. West Conshohocken (PA): American Society for Testing and Materials; 2000. p. 305–317

16. Wilson CD. Fracture Toughness Testing with Notched Round Bars. Knoxville (TN): The University of Tennessee, PhD Thesis; 1997 Aug. 106p

17. Chaphalkar PP. Fracture Toughness Measurement for Aluminium 6061-T6 using Notched Round Bars. Sydney (NSW): School of Mechanical and Manufacturing Engineering, UNSW Australia (The University of New South Wales), Coursework Masters Thesis; 2014 Nov 25. 121p

18. ASM International: ASM Aerospace Specification Metals Inc. Aluminum 6061-T6; 6061-T651 [Internet]. Materials Park (OH): American Society of Materials; c1913-2017 [cited 2014 Nov 6]. Available from: http://asm.matweb.com/search/SpecificMaterial.asp?bassnum=MA6061t6.

19. Australian Standard AS 1391—2007 (R2017) (Incorporating Amendment No. 1, 2012). Metallic Materials—Tensile Testing at Ambient Temperature. Sydney (NSW): Standards Australia; 2007 Jul 12. 64p

20. Young WC, Budynas RG. Roark's Formulas for Stress and Strain. 7th ed. New York: McGraw-Hill; 2002. 852p

21. Irwin GR. Structural aspects of brittle fracture. *Appl Mater Res.* 1964 Apr;3(2):65-81.

22. Shabara MAN, El-Domiaty AA, Al-Ansary MD. Estimation of plane strain fracture toughness from circumferentially bluntly notched round-bar specimens. *Eng Fract Mech.* 1996 Jul;54(4):533-541.

23. Vanian GG, Hellier AK, Zarrabi K, Prusty BG. Fracture toughness determination for aluminium alloy 2011-T6 using tensile notched round bar (NRB) test pieces. *Int J Fract.* 2013 May;181(1):147-154.

24. Hertzberg RW. Microstructural aspects of fracture toughness. Chapter 10 in: Deformation and Fracture Mechanics of Engineering Materials. New York: John Wiley & Sons; 1976. p. 326–327